Mutagenesis vol. 28 no. 3 pp. 263–270, 2013
Advance Access publication 5 February 2013
doi:10.1093/mutage/ges080

T-cell-specific deletion of *Mof* blocks their differentiation and results in genomic instability in mice

Arun Gupta[1,2], Clayton R. Hunt[1,2], Raj K. Pandita[2,3], Juhee Pae[4], K. Komal[5], Mayank Singh[1], Jerry W. Shay[3], Rakesh Kumar[1,2], Kiyoshi Ariizumi[4], Nobuo Horikoshi[1], Walter N. Hittelman[6], Chandan Guha[7], Thomas Ludwig[8] and Tej K. Pandita[1,2,*]

[1]Department of Radiation Oncology, UT Southwestern Medical Center, Dallas, TX 75229, USA, [2]Washington University School of Medicine, St Louis, MO 63108, USA, [3]Department of Cell Biology, UT Southwestern Medical Center, Dallas, TX 75229, USA, [4]Department of Dermatology, UT Southwestern Medical Center, Dallas, TX 75229, USA, [5]All India Institute of Medical Sciences, Delhi, India, [6]Department of Experimental Therapeutics, MD Anderson Cancer Center, Houston, TX 77030, USA, [7]Department of Radiation Oncology, Albert Einstein College of Medicine, Bronx, NY 10461, USA, [8]Institute for Cancer Genetics, Columbia University, New York, NY 32001, USA and [9]Department of Molecular and Cellular Biochemistry, Ohio State University Wexner Medical Center, Columbus, OH 43210, USA

*To whom correspondence should be addressed. Department of Radiation Oncology, UT Southwestern Medical Center, 2201 Inwood Road, Dallas, TX 75390, USA. Tel: 1-214-648-1918; Fax: 1-214-648-8995;
Email: tej.pandita@utsouthwestern.edu

Received on October 20, 2012; revised on December 11, 2012; accepted on December 12, 2012

Ataxia telangiectasia patients develop lymphoid malignancies of both B- and T-cell origin. Similarly, ataxia telangiectasia mutated (Atm)-deficient mice exhibit severe defects in T-cell maturation and eventually develop thymomas. The function of ATM is known to be influenced by the mammalian orthologue of the *Drosophila MOF* (males absent on the first) gene. Here, we report the effect of T-cell-specific ablation of the mouse Mof (*Mof*) gene on leucocyte trafficking and survival. Conditional *Mof*$^{Flox/Flox}$ (*Mof*$^{F/F}$) mice expressing Cre recombinase under control of the T-cell-specific Lck proximal promoter (*Mof*$^{F/F}$*/Lck-Cre*$^{+}$) display a marked reduction in thymus size compared with *Mof*$^{F/F}$*/Lck-Cre*$^{-}$ mice. In contrast, the spleen size of *Mof*$^{F/F}$*/Lck-Cre*$^{+}$ mice was increased compared with control *Mof*$^{F/F}$*/Lck-Cre*$^{-}$ mice. The thymus of *Mof*$^{F/F}$*/Lck-Cre*$^{+}$ mice contained significantly reduced T cells, whereas thymic B cells were elevated. Within the T-cell population, CD4^{+}CD8^{+} double-positive T-cell levels were reduced, whereas the immature CD4^{-}CD8^{-} double-negative (DN) population was elevated. Defective T-cell differentiation is also evident as an increased DN3 (CD44^{-}CD25^{+}) population, the cell stage during which T-cell receptor rearrangement takes place. The differentiation defect in T cells and reduced thymus size were not rescued in a p53-deficient background. Splenic B-cell distributions were similar between *Mof*$^{F/F}$*/Lck-Cre*$^{+}$ and *Mof*$^{F/F}$*/Lck-Cre*$^{-}$ mice except for an elevation of the κ light-chain population, suggestive of an abnormal clonal expansion. T cells from *Mof*$^{F/F}$*/Lck-Cre*$^{+}$ mice did not respond to phytohaemagglutinin (PHA) stimulation, whereas LPS-stimulated B cells from *Mof*$^{F/F}$*/Lck-Cre*$^{+}$ mice demonstrated spontaneous genomic instability. Mice with T-cell-specific loss of MOF had shorter lifespans and decreased survival following irradiation than did *Mof*$^{F/F}$*/Lck-Cre*$^{-}$ mice. These observations suggest that Mof plays a critical role in T-cell differentiation and that depletion of Mof in T cells reduces T-cell numbers and, by an undefined mechanism, induces genomic instability in B cells through bystander mechanism. As a result, these mice have a shorter lifespan and reduced survival after irradiation.

Introduction

Males absent on the first (MOF) was initially discovered as a dosage compensation gene in *Drosophila*. MOF belongs to the MYST family of acetyltransferases and is a histone acetyltransferase (HAT) that acetylates chromatin specifically at histone H4 lysine 16 (H4K16). Depletion of MOF in *Drosophila* (1), as well as in human and mouse cells, results in the loss of acetylation at H4K16 (2–6), suggesting that the highly conserved MOF protein may be the major HAT acting on histone H4 at K16. MOF has been associated with acute myeloid leukaemia (AML) and transcriptional silencing in *Saccharomyces cerevisiae* (*SAS2* and *YBF2/SAS3*). MOF also interacts with the human immunodeficiency virus Tat-interactive protein (TIP60) (7–9). We previously reported a higher frequency of residual DNA double-strand breaks and chromosome aberrations in cells expressing a HAT-dead human MOF after cellular exposure to ionising radiation (IR) (6,10). Additional studies indicate MOF plays a critical role in oogenesis, oncogenesis, DNA damage repair and survival of post-mitotic Purkinje cells (2,5,10). Chromosomal translocations that alter the activity of chromatin-modifying enzymes are repeatedly found associated with different forms of leukaemia indicating the importance of epigenetic regulation in haematopoiesis. One of these chromatin-modifying enzymes, the monocytic leukaemia zinc finger (MOZ or recently renamed as KAT6a3) protein, was first identified through positional cloning of a t(8;16)(p11;p13) translocation of the CREB-binding protein gene in AML (11).

MOF affects ATM function, the gene responsible for the disease ataxia telangiectasia (A-T). Patients with mutated ATM have ~5-fold increased risk of developing leukaemia or lymphoblastic lymphomas and ~10% of A-T patients develop lymphoid malignancies (12,13) of either B-cell or T-cell origin (14). Similarly, Atm-deficient mice exhibit severe defects in T-cell maturation and develop thymomas (15). As MOF regulates ATM function, we sought to determine the effect of Mof depletion on T-cell maturation. Since global Mof ablation results in early embryonic lethality (5), we employed a conditional murine system in which the Lck proximal promoter drives T-cell-specific expression of Cre recombinase (*Mof*$^{F/F}$*/Lck-Cre*$^{+}$ mice) to determine the role of Mof in T-cell development.

Materials and methods

Generation of T-cell-specific Mof-deficient mice

The details for generation of targeting vectors for the *Mof* locus used for an *in vivo* deletion of the *Mof* gene in mice and the conditional *Mof* allele were described recently (5,10). W9.5 ES cells were electroporated with the construct

to generate *Mof*$^{flox/+}$ cells and the details for generation of *Mof*$^{flox/+}$/*Rosa26*$^{creERT2/+}$ and *Mof*$^{Dflox/flox}$/*Rosa26*$^{creERT2/+}$ ES cell clones have been described (5,10).

To inactivate Mof specifically in T cells, conditional *Mof*$^{flox/flox}$ (*Mof*$^{F/F}$) mice were crossed with mice expressing Cre recombinase under the control of the Lck proximal promoter (16) to generate MofF/F/Lck-Cre+ mice. Genotyping of mice was performed as described previously (5,10). Animal care and treatments were performed in accordance with the National Institutes of Health guidelines at Washington University School of Medicine, St Louis, MO and Columbia University, New York.

Leucocyte isolation and flow cytometric analysis

For leucocyte isolation and flow cytometric analysis, cell suspensions prepared from fresh thymus and spleen were negatively enriched for T cells through magnetic bead depletion of B cells, NK cells, dendritic cells, granulocytes, monocytes/macrophases and erythrocytes. For immunophenotyping, T cells were stained with specific primary-conjugated antibodies and analysed by Dickinson FACSCalibur flow. CD4$^-$CD8$^-$ double-negative (DN) thymocyte subset purification was performed by staining unfractionated thymocytes with a fluorescein isothiocyanate (FITC)-labelled lineage-specific antibodies for CD4 and CD8. Spleen cells from *Mof*$^{flox/flox}$/*Lck-Cre*$^+$ mice and *Mof*$^{flox/flox}$/*Lck-Cre*$^-$ mice were depleted of T cells, then cultured in RPMI 1640 medium supplemented with 10% fetal calf serum in the presence of 4 pg/ml of lipopolysaccharide (LPS) to stimulate B cells. T cells were stimulated with phytohaemagglutinin (PHA). After 48 or 72 h of culture, colcemid was added and metaphases were prepared and analysed as described previously (17,18). To determine whether metaphases are from first (I), second (II) or third (III) cell cycle post-LPS stimulation, cells were incubated with BrdU and cell cycle (I, II, III) was determined as described previously (17). Metaphase bone marrow cells were prepared from mice 4 h after administering colcemid. Telomere fluorescence *in situ* hybridization (FISH) was performed as described previously (19–21).

Micronuclei analysis and ratio of normochromatic to polychromatic erythrocytes

Frequency of micronucleus and the ratio of normochromatic to polychromatic erythrocytes were determined by previously described procedures (18,21,22). Briefly, bone marrow smears from the age-matched *Mof*$^{F/F}$/*Lck-Cre*$^+$ and *Mof*$^{F/F}$/*Lck-Cre*$^-$ mice with and without treatment of mitomycin C were prepared, and the stained smears were examined to determine the incidence of micronucleated cells in 1800 polychromatic erythrocytes and the ratio of normochromatic to polychromatic erythrocytes for each animal, which were repeated three times.

Statistical analysis

Data are expressed as the means ± standard deviations from three to four experiments. Statistical comparison of means was performed by the Student's *t*-test.

Results and discussion

Most of the A-T patients suffer from immune defects and MOF influences ATM function (6,23,24). Global Mof inactivation results in early embryonic lethality in mice (5). Therefore, we generated mice with T-cell-specific Mof deletion by breeding conditional *Mof*$^{Flox/Flox}$ (*Mof*$^{F/F}$) mice (10) with transgenic mice expressing Cre recombinase under control of the Lck proximal promoter to generate *Mof*$^{F/F}$/Lck-Cre$^+$ mice. This approach provided a well-defined system for determining the role of Mof in leucocyte biology through Cre-mediated deletion in developing T cells (16). Lck is a non-receptor protein tyrosine kinase required for signal transduction via the T-cell antigen receptor and the Lck proximal promoter is activated at the DN1 (CD25$^-$CD44$^+$) to DN2 (CD25$^+$CD44$^+$) T-cell lineage stage. The production and 'education' of T cells, which are critical for the adaptive immune system, occur in the thymus, which provides an inductive environment for the development of T lymphocytes from haematopoietic progenitor cells.

T-cell-specific ablation of Mof had a major effect on the thymus and spleen (Figure 1A–D), *Mof*$^{F/F}$/*Lck-Cre*$^+$ mice had consistently smaller thymi (approximately half of the size relative to their body weight) than those of *Mof*$^{F/F}$/*Lck-Cre*$^-$ mice and the differences observed (at either 3 or 12 weeks of age) are statistically significant (Figure 1B and D). In contrast, spleen size in *Mof*$^{F/F}$/*Lck-Cre*$^+$ mice is consistently larger relative to body weight compared with *Mof*$^{F/F}$/*Lck-Cre*$^-$ mice (Figure 1B and D) with differences being more pronounced at 12 weeks of age. The size reduction of the thymus was not p53-dependent since *Mof*$^{F/F}$/*Lck-Cre*$^+$ mice generated in a p53-null background mice still displayed the reduced thymus size phenotype seen in *Mof*$^{F/F}$/*Lck-Cre*$^+$ mice (Figure 1E and F). Irrespective of p53 status, the ratio of thymus size is reduced and spleen increased in 12-week-old compared with 3-week-old *Mof*$^{F/F}$/*Lck-Cre*$^+$ mice. A reduction in thymus size has also been observed in mice with inactivated MOZ, another MYST family member, where both B and T cells were affected (25). Here, we observe that thymus size is affected by T-cell-specific inactivation of Mof. It is known that thymus function is eventually taken over by the spleen in adults so the increase in spleen size seen here might be due to defective T-cell development, which results in spleen hypertrophy in *Mof*$^{F/F}$/*Lck-Cre*$^+$ mice (Figure 1).

Immunostaining with Mof antibody of thymus and spleen tissue sections prepared from *Mof*$^{F/F}$/*Lck-Cre*$^-$ mice detected positive staining for Mof in both tissues (Figure 2A). Furthermore, when T and B cells from thymus and spleen of *Mof*$^{F/F}$/*Lck-Cre*$^+$ and *Mof*$^{F/F}$/*Lck-Cre*$^-$ mice were enriched and examined for Mof and H4K16ac levels, both were significantly reduced in T cells from *Mof*$^{F/F}$/*Lck-Cre*$^+$ mice compared with T cells from *Mof*$^{F/F}$/*Lck-Cre*$^-$ mice (Figure 2B). However, no reduction in Mof or H4K16ac levels was observed in B cells of *Mof*$^{F/F}$/*Lck-Cre*$^+$ mice (Figure 2B).

To investigate potential immune system abnormalities, we performed flow cytometry analysis of thymocytes and splenocytes from *Mof*$^{F/F}$/*Lck-Cre*$^+$ and *Mof*$^{F/F}$/*Lck-Cre*$^-$ mice. Fewer cells were collected from thymi of *Mof*$^{F/F}$/*Lck-Cre*$^+$ mice in comparison with controls, which is consistent with the smaller organ size in *Mof*$^{F/F}$/*Lck-Cre*$^+$ mice (Figure 1). Thymocytes from 12-week-old *Mof*$^{F/F}$/*Lck-Cre*$^+$ mice had a significant reduction in total T-cell population compared with *Mof*$^{F/F}$/*Lck-Cre*$^-$ mice (Figure 3A(a)). T cells from *Mof*$^{F/F}$/*Lck-Cre*$^+$ mice displayed a reduction of mature T cells (CD4$^+$CD8$^+$) and an accumulation of immature DN T cells (CD4$^-$CD8$^-$) (Figure 3A(c)). Further analysis revealed that T-cell development was retarded after *Mof* gene disruption at the DN3 (CD44$^-$CD25$^+$) stage, where T-cell receptor rearrangements are processed for β-receptor selection, and following DN4 stage (CD44$^-$CD25$^-$). Defective T-cell receptor rearrangement is a phenotype observed in A-T patients as well as in Atm-deficient mice (15,26,27), thus, Mof expression appears to be critical for T-cell development. Reduced T-cell populations were also observed in spleen (Figure 3B(a)) especially in the cytotoxic T-cell (CD4$^-$CD8$^+$) population (Figure 3B(c)).

While the T-cell population decreased, the thymic B-cell population was increased in *Mof*$^{F/F}$/*Lck-Cre*$^+$ mice (Figure 3A(a)). A similar B-cell increase was observed as a result of apoptosis in the thymus (28), suggesting the decreased thymus size in *Mof*$^{F/F}$/*Lck-Cre*$^+$ mice could be due, at least in part, to apoptotic elimination of immature T cells. However, when we examined *Mof*$^{F/F}$/*Lck-Cre*$^+$ mice in a p53-null background (Figure 4), there was no normalisation of thymus and spleen size (Figure 1E and F), nor did p53 inactivation affect the altered T- and B-cell distribution observed in Mof-deficient mice (Figure 4). In thymus, total T cells were reduced with increasing immature CD4$^-$CD8$^-$ DN and reducing CD4$^+$CD8$^+$ double-positive populations (Figure 4A(b)), whereas thymic B

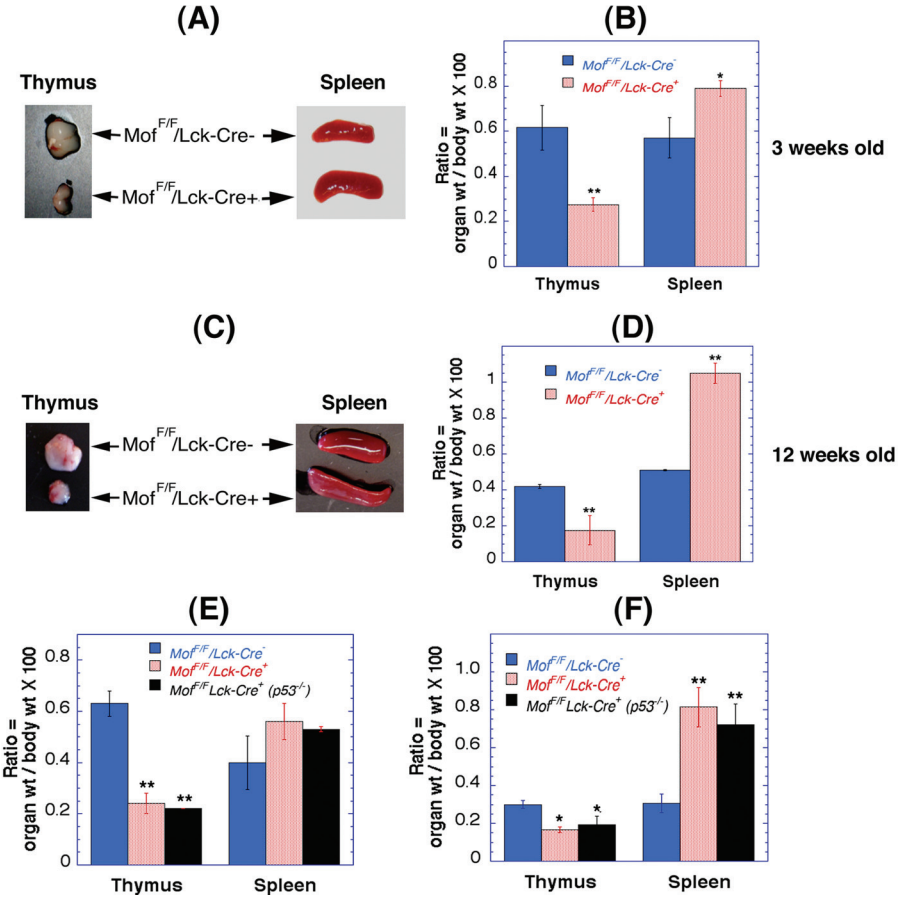

Fig. 1. Effect of T-cell-specific Mof inactivation on thymus and spleen size. (**A**) Thymus and spleen from 3-week-old *Mof*$^{F/F}$*/Lck-Cre*$^{+}$ and *Mof*$^{F/F}$*/Lck-Cre*$^{-}$ mice. (**B**) Histogram of the weight ratios of thymus and spleen to mouse body weight. The differences in thymus as well as spleen size in *Mof*$^{F/F}$*/Lck-Cre*$^{+}$ and *Mof*$^{F/F}$*/Lck-Cre*$^{-}$ mice are statistically significant. (**C**) Thymus and spleen of 12-week-old *Mof*$^{F/F}$*/Lck-Cre*$^{+}$ and *Mof*$^{F/F}$*/Lck-Cre*$^{-}$ mice. (**D**) Histogram showing the ratio of thymus and spleen to body weight. The thymus size is relatively smaller and spleen size is larger. The differences in thymus as well as spleen size in *Mof*$^{F/F}$*/Lck-Cre*$^{+}$ and *Mof*$^{F/F}$*/Lck-Cre*$^{-}$ mice are statistically significant. (**E** and **F**) Thymus and spleen size in p53-null background of *Mof*$^{F/F}$*/Lck-Cre*$^{+}$ and *Mof*$^{F/F}$*/Lck-Cre*$^{-}$ mice (E: 3 weeks old and F: 12 weeks old). $*P < 0.05$ and $**P < 0.001$ determined by the chi-square test.

cells were increased (Figure 4A(a)). In spleen, the number of mature B cells was unchanged (Figure 4B(a)), whereas total T cells were reduced (Figure 4B(b)). In sum, p53 does not play a significant role in the reduced thymus size or defective T-cell development seen in Mof-deficient mice.

Precursor B and T cells are produced in the bone marrow. To determine whether inactivation of Mof in T cells has any effect on bone marrow erythrocytes, we compared the number of micronucleated cells per 1800 polychromatic erythrocytes and the ratio of normochromatic to polychromatic erythrocytes in *Mof*$^{F/F}$*/Lck-Cre*$^{+}$ and *Mof*$^{F/F}$*/Lck-Cre*$^{-}$ mice with or without treatment of mitomycin C. No significant differences were found between the two genotypes (Table I). This is reasonable since the Lck proximal promoter driving Cre recombinase is activated in thymus, thus T-cell precursors in bone marrow are likely express Mof gene.

To determine the cause for the T-cell differentiation blockage in *Mof*$^{F/F}$*/Lck-Cre*$^{+}$ mice, thymocytes were examined for genomic integrity. We have recently shown that genomic integrity as well as the DNA damage response can be influenced by H4K16ac levels (2) as the H4K16ac modification structurally constrains the formation of higher-order chromatin (29), perhaps by inducing an open chromatin configuration that is more readily accessible to transcription as well as DNA repair proteins. H4K16ac is also critical for protein–protein interactions (29), and reduced levels of H4K16ac correlate with a defective DNA damage response (2). Since thymus or blood T cells from *Mof*$^{F/F}$*/Lck-Cre*$^{+}$ mice responded very poorly to PHA treatment for blastoid formation (data not shown), we collected thymocytes to examine nuclear morphology. Interestingly, a significant fraction (>14%) of T cells from *Mof*$^{F/F}$*/Lck-Cre*$^{+}$ mice displayed chromatin blebbing and disintegration of the nucleus (Figure 5A and B), similar to the situation observed in MOF-depleted HeLa cells (4) as well as to the chromatin condensation observed in Mof-deleted post-mitotic neuronal Purkinje cells (10). These observations suggest that failure to maintain genomic integrity could be the major cause for defective T-cell development.

Precursor T cells mature in the thymus and helper T cells are known to release factors such as lymphokines that enhance B-cell blastoid formation as well as differentiation (30,31). As shown in Figures 1 and 3, depletion of Mof in T cells results in spleen enlargement and possibly abnormal clonal expansion of B cells. To determine the effect of Mof depletion on T cells, we compared the status of T-cell blastoid transformation in *Mof*$^{F/F}$*/Lck-Cre*$^{+}$ and *Mof*$^{F/F}$*/Lck-Cre*$^{-}$ mice. PHA treatment produced minimal blastoid formation or metaphases in T cells from the thymus or spleen of *Mof*$^{F/F}$*/Lck-Cre*$^{+}$ mice, whereas both blastoid and metaphases were seen in the cells from the *Mof*$^{F/F}$*/Lck-Cre*$^{-}$ mouse thymus or spleen, suggesting that Mof is important for mitogen-induced replication of T cells (data not shown).

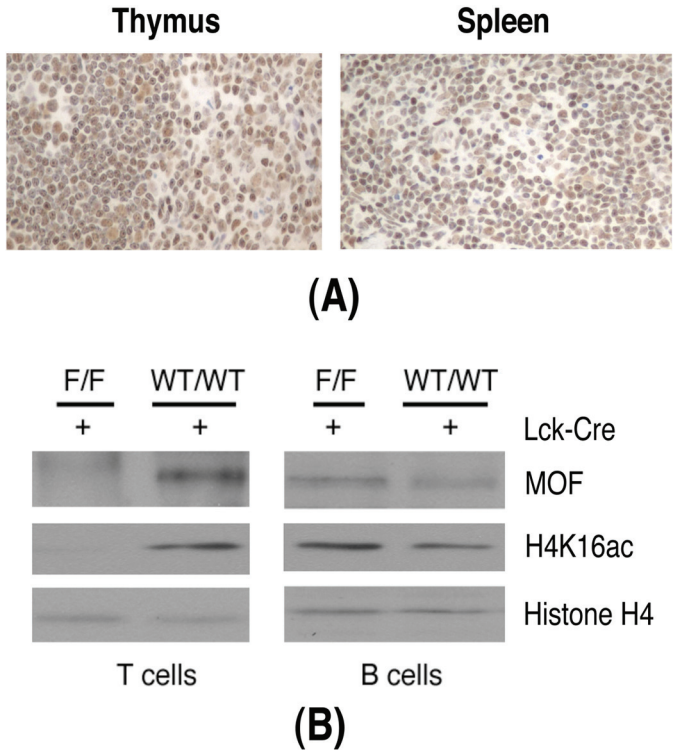

Fig. 2. Immunostaining and western blot detection of Mof expression. (**A**) Immunostaining of Mof in thymus and spleen of 3-week-old control mice. (**B**) Western blot analysis of Mof and H4K16ac levels in thymus T cells and spleen B cells from *Mof*$^{F/F}$*/Lck-Cre*$^{+}$ and *Mof*$^{F/F}$*/Lck-Cre*$^{-}$ mice.

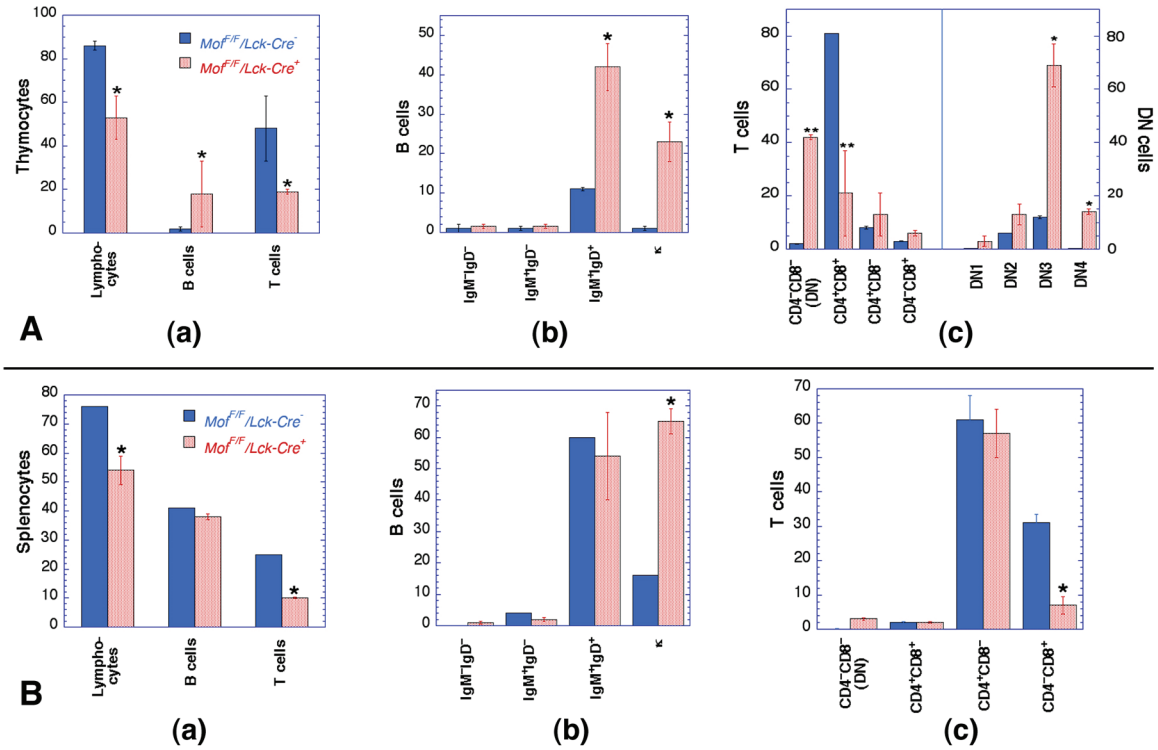

Fig. 3. Analysis of thymus and spleen lymphocytes in *Mof*$^{F/F}$*/Lck-Cre*$^{+}$ and *Mof*$^{F/F}$*/Lck-Cre*$^{-}$ mice. (**A**) Comparison of lymphocytes from (**a**) *Mof*$^{F/F}$*/Lck-Cre*$^{+}$ thymus indicating a significant reduction in total lymphocytes and pan T cells ($CD3^{+}CD5^{+}$) but increased pan B cells ($B220^{+}$) levels; (**b**) thymic B cells from *Mof*$^{F/F}$*/Lck-Cre*$^{+}$ mice indicate a significant increase in mature B cells ($IgM^{+}IgD^{+}$) with an unusually high clonal (κ light-chain) expansion ratio (**κ**); and (**c**) thymic T cells from *Mof*$^{F/F}$*/Lck-Cre*$^{+}$ indicating an early developmental defect, increased population of $CD4^{-}CD8^{-}$ (DN) T cells as well as statistically significant decreased $CD4^{+}CD8^{+}$ T cells. DN population was further classified into DN1 ($CD44^{+}CD25^{-}$), DN2 ($CD44^{+}CD25^{+}$), DN3 ($CD44^{-}CD25^{+}$) and DN4 ($CD44^{-}CD25^{-}$) populations and T cells from *Mof*$^{F/F}$*/Lck-Cre*$^{+}$ accumulated in DN3 and DN4. (**B**) Comparison of cells from spleen (**a**) statistically significant reduction in total lymphocytes and T cells, whereas total B-cell number was unchanged; (**b**) difference in B cells, mature B cell ($IgM^{+}IgD^{+}$) was unchanged; however, abnormal κ light-chain clonal expansion was observed; (**c**) difference in splenic T cells, the number of helper T cells ($CD4^{+}CD8^{-}$) was unchanged; however, cytotoxic T-cells ($CD4^{-}CD8^{+}$) level was reduced. *$P < 0.05$ and **$P < 0.001$ determined by the chi-square test.

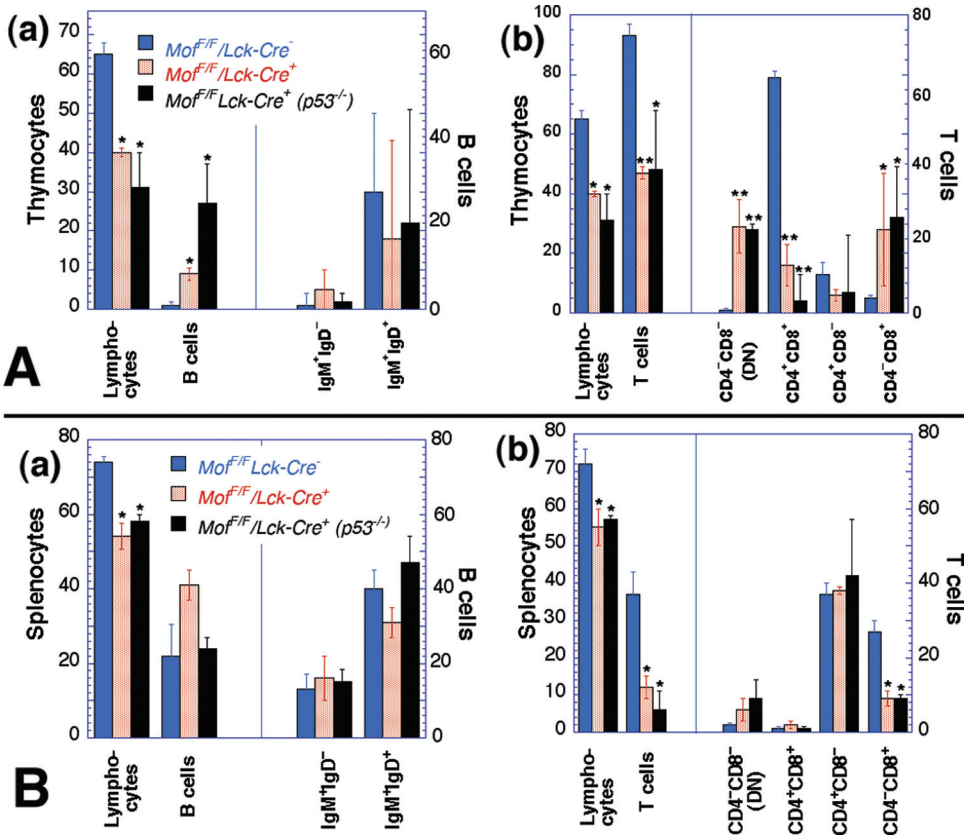

Fig. 4. Effect of p53-null status on thymic and splenic cell populations in *Mof*$^{F/F}$*/Lck-Cre*$^{+}$ mice. (**A**) Comparison of cells from thymus (**a**) B cells and (**b**) T cells present no significant differences in cell types between p53-null and wild-type background of *Mof*$^{F/F}$*/Lck-Cre*$^{+}$ mice; however, significant differences were observed between *Mof*$^{F/F}$*/Lck-Cre*$^{+}$ and *Mof*$^{F/F}$*/Lck-Cre*$^{-}$ mice as described in Figure 3. (**B**) Comparison of cells from spleen. (**a**) B cells and (**b**) T cells present no significant differences in cell types of p53-null and wild-type background *Mof*$^{F/F}$*/Lck-Cre*$^{+}$ mice; however, some differences were observed between *Mof*$^{F/F}$*/Lck-Cre*$^{+}$ and *Mof*$^{F/F}$*/Lck-Cre*$^{-}$ mice as described in Figure 3. *$P < 0.05$ and **$P < 0.001$ determined by the chi-square test.

Next, to determine whether T-cell-specific inactivation of Mof also affects B-cell proliferation, splenocytes and whole white blood cells were treated with LPS, to specifically stimulate B cells. About ~7% of metaphases in LPS-treated splenic B cells of *Mof*$^{F/F}$*/Lck-Cre*$^{+}$ mice (3 weeks old) had chromosomes with loss of telomere signals, as detected by telomere-specific FISH (Figure 5C, red arrows) and chromosome fragments (Figure 5C, white arrow). No such corresponding chromosomal defects were observed in *Mof*$^{F/F}$*/Lck-Cre*$^{-}$ mice. Also, ~8% of metaphases from spleen-derived B cells from *Mof*$^{F/F}$*/Lck-Cre*$^{+}$ mice displayed chromosome end-to-end association (Figure 5D, yellow arrows) not seen in *Mof*$^{F/F}$*/Lck-Cre*$^{-}$ mice. Similar chromosome end-to-end associations have been reported previously in cells derived from A-T patients (19,32). In addition, B cells from spleens of older (12 or 15 weeks old) *Mof*$^{F/F}$*/Lck-Cre*$^{+}$ mice also displayed a high frequency of chromosome fragments, loss of telomere signals and telomere fusions resulting in Robertsonian mutations (Figure 5E–H).

Table I. Number of micronucleated polychromatic erythrocytes and the ratio of normochromatic to polychromatic erythrocytes in bone marrow smears after intraperitoneal administration of mitomycin C

Genotype	Treatment	Number of micronuleated cells/1800 polychromatic erythrocytes/mouse		Ratio of normochromatic to polychromatic erythrocytes	
	Mitomycin C (mg/kg body weight)	Mean	Range	Mean	Range
Mof$^{F/F}$*/Lck-Cre*$^{-}$	0	1.20	0–3.90	1.62	0.51–3.40
	5	80.30	35–127	22.50	5.10–51.60
Mof$^{F/F}$*/Lck-Cre*$^{+}$	0	1.28	0–4.00	1.68	0.54–3.51
	5	82.32	34–130	23.70	5.21–53.28

The mechanistic basis for B-cell genomic instability in mice with T-cell-specific Mof depletion was further examined by determining where in the cell cycle phase-specific chromosomal aberrations could occur through a bystander mechanism (33–35). B cells stimulated with LPS were labelled with BrdU and metaphase cells collected after 48 h of incubation. Cell cycle phase-specific chromosome aberrations were ascertained based on the frequency of chromosomal and chromatid-type aberrations observed at metaphase. G_1-specific aberrations detected at metaphase are mostly of the chromosomal type and include a high frequency of dicentrics (21,36,37). S-phase-type aberrations detected at metaphase are chromosomes and chromatid-type aberrations along with tri- or quadriradials, whereas G_2-phase-type aberrations are only chromatid type. After stimulation, only chromosome-type aberrations were observed at first metaphase as determined by Fluorescence Plus Giemsa technique as described previously (17). The possibility of missing chromatid aberrations arising during S phase was minimal as no metaphase cells with both chromatid DNA strands labelled with BrdU were detected by the described procedure (17,18). These results suggest that the genomic instability

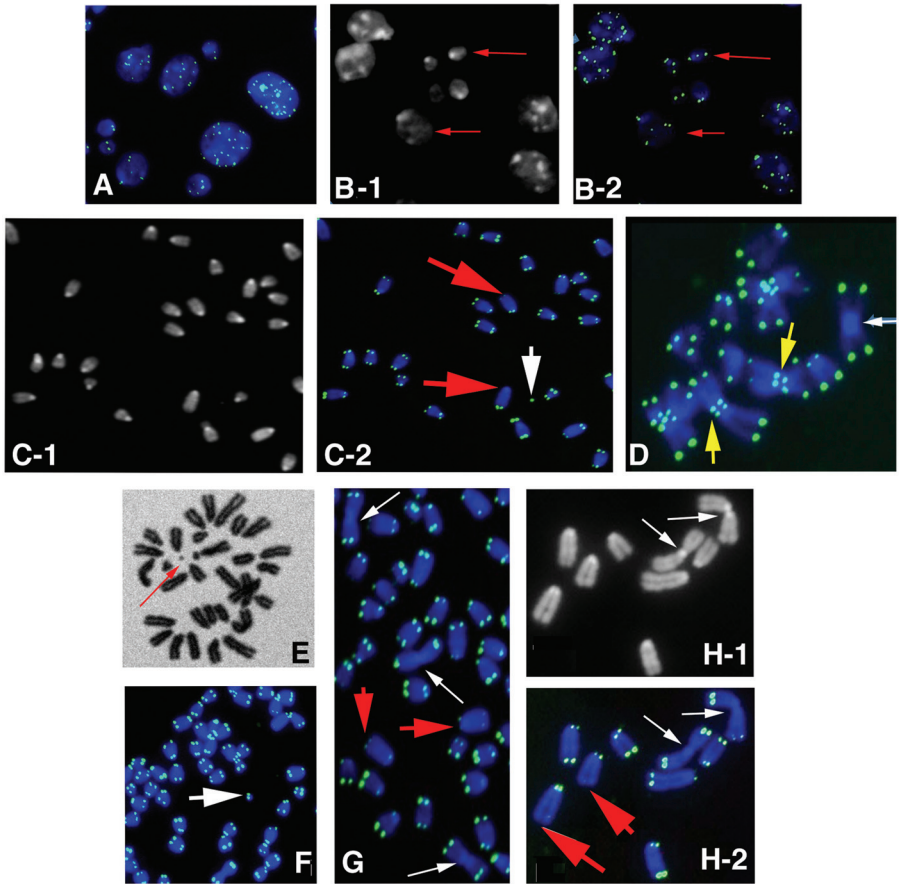

Fig. 5. Genomic instability of T cells and B cells in *Mof*$^{F/F}$*/Lck-Cre*$^{+}$ mice. (**A**) T cells from thymus of 3-week-old mice showing nuclei of different sizes. Telomere signals (green) are detected by using telomere-specific probe. DNA was stained with DAPI (4′,6-diamidino-2-phenylindole) (blue). (**B**) T cells from thymus of 12-week-old mice. (B-1) DAPI staining and (B-2) telomere signals detected by FISH. Red arrows indicate the fragmented nuclei with or without telomere signals. (**C**) Metaphases from B cells of 3-week-old mice (C-1) DAPI staining and (C-2) telomere FISH staining, red arrows showing loss of telomere signals and white arrow showing a fragment with telomere signal. (**D**) Metaphase from 6-week-old mouse B cells showing chromosome end-to-end associations (yellow arrow) and telomere fusion leading to Robertsonian mutation (white arrow). (**E**) Giemsa staining of metaphase from 12-week-old mouse B cells showing chromosome fragments. (**F**) Metaphase of B cells showing fragment with telomere signal and (**G**) metaphase of B cells with loss or reduced telomere signal (red arrows) and high frequency of telomere fusions (white arrows). (**H**) Metaphase segment from 15-week-old mouse B cells showing telomere fusions leading to Robertsonian mutations (H-1) DAPI staining, white arrows showing chromosome end fusions and (H-2) telomere FISH showing loss of telomere signal (red arrows) and telomere fusions without any telomere signals (white arrows).

observed in B cells arises during the G_0/G_1 phase of the cell cycle by LPS stimulation since no micronuclei were observed in untransformed/unstimulated B cells from *Mof*$^{F/F}$*/Lck-Cre*$^{+}$ mice. Since B-cell numbers in spleen did not show a reduction (Figures 3B and B), these chromosomal instabilities could be associated with abnormal clonal expansion (Figure 3B(b)).

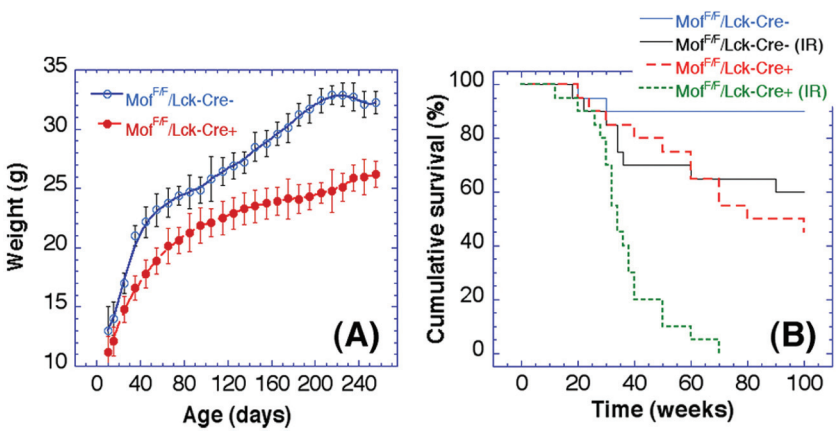

Fig. 6. Effect of T-cell-specific Mof depletion on weight and post-irradiation survival. (**A**) Body weight and (**B**) survival after 3 Gy IR exposure of *Mof*$^{F/F}$*/Lck-Cre*$^{+}$ and *Mof*$^{F/F}$*/Lck-Cre*$^{-}$ mice. The differences in the weight and survival of *Mof*$^{F/F}$*/Lck-Cre*$^{+}$ and *Mof*$^{F/F}$*/Lck-Cre*$^{-}$ mice are modest, but statistically significant ($P < 0.05$ determined by the chi-square test). The cumulative survival was plotted according to Kaplan–Meier analysis.

To determine whether the genomic instability seen in B cells from spleen or thymus could be originating from bone marrow precursor B cells, we analysed metaphases in bone marrow cells from *Mof*$^{F/F}$*/Lck-Cre*$^{+}$ and *Mof*$^{F/F}$*/Lck-Cre*$^{-}$ mice and found no difference in genomic stability, suggesting that Mof depletion in T cells seen in the thymus had no effect on the precursor cells.

We next determined whether the immunological alternations observed in *Mof*$^{F/F}$*/Lck-Cre*$^{+}$ mouse impacted growth by comparing the body weight of *Mof*$^{F/F}$*/Lck-Cre*$^{+}$ and *Mof*$^{F/F}$*/Lck-Cre*$^{-}$ mice. A significant decrease in body weight of *Mof*$^{F/F}$*/Lck-Cre*$^{+}$ mice was observed compared with *Mof*$^{F/F}$*/Lck-Cre*$^{-}$ mice (Figure 6A). In addition, *Mof*$^{F/F}$*/Lck-Cre*$^{+}$ mice had a shortened lifespan compared with *Mof*$^{F/F}$*/Lck-Cre*$^{-}$ mice (Figure 6B). Since *Mof*$^{F/F}$*/Lck-Cre*$^{+}$ mice display genomic instability of lymphocytes, we examined whether the mice were radiosensitive. Mice (4 weeks of age) were treated with 3 Gy of IR and survival monitored for up to 100 weeks. Long-term survival of irradiated *Mof*$^{F/F}$*/Lck-Cre*$^{+}$ mice was significantly decreased compared with *Mof*$^{F/F}$*/Lck-Cre*$^{-}$ mice (Figure 6B). Taken together, the results indicate that mice with Mof-deficient T cells have compromised immune systems and manifest growth retardation as well as increasing radiation sensitivity.

We report here that T-cell-specific deletion of the *Mof* gene results in a smaller thymus and larger spleen and a blockage in T-cell differentiation at the stage during which T-cell receptor rearrangement normally occurs, which may correlate with genomic instability. Interestingly, loss of Mof in T cells also induces a genomic instability phenotype in B cells. Mice with Mof-null T cells had a reduced body weight as well as a reduced lifespan and demonstrated higher sensitivity to irradiation. This is similar to the situation in severe combined immunodeficient mice where a germ-line mutation in the DNA-PKcs gene blocks T- and B-cell development and there is elevated sensitivity to radiation (38). Since MOF influences ATM functions in response to DNA damage (6,39), the results suggest the mice have a defect in Atm-signalling pathway in T cells and thus demonstrate T-cell development defects similar to those observed in A-T patients and Atm-null mice. In addition, mice with T-cell-specific MOF inactivation display high genomic instability in B cells providing a valuable means for understanding the role of chromatin-modifying factors, such as MOF, in the development of leukaemias and lymphomas. T cells are known to be important for B-cell functions; however, what factor(s) that are released by T cells induce genomic instability in B cells is not known. The identity of such factor(s) responsible for the bystander effects remains an interesting question to be answered.

Funding

National Institutes of Health/National Cancer Institute (R01CA123232, R01CA129537, R01CA154320, U19A1091175, R13CA130756, P01CA97403 and R01CA137023).

Acknowledgements

We thank members of the T.K.P. laboratory and K. Choi for helpful discussions and suggestions.

Author contributions: A.G., C.R.H., T.L. and T.K.P. designed research; A.G., J.P., R.K., C.R.H. and R.K.P. performed research; T.L., W.N.H. and C.G. contributed new reagents/analytic tools; J.W.S., J.W.S., W.N.H., K.K. and T.K.P. analysed data; and A.G., C.R.H., C.G., J.W.S., T.L., K.A., N.H. and T.K.P. wrote the paper.

Conflict of interest statement: None declared.

References

1. Bhadra, M. P., Horikoshi, N., Pushpavallipvalli, S. N. *et al.* (2012) The role of MOF in the ionizing radiation response is conserved in Drosophila melanogaster. *Chromosoma*, **121**, 79–90.
2. Sharma, G. G., So, S., Gupta, A. *et al.* (2010) MOF and histone H4 acetylation at lysine 16 are critical for DNA damage response and double-strand break repair. *Mol. Cell. Biol.*, **30**, 3582–3595.
3. Smith, A. T., Tucker-Samaras, S. D., Fairlamb, A. H. and Sullivan, W. J., Jr. (2005) MYST family histone acetyltransferases in the protozoan parasite Toxoplasma gondii. *Eukaryot. Cell*, **4**, 2057–2065.
4. Taipale, M., Rea, S., Richter, K., Vilar, A., Lichter, P., Imhof, A. and Akhtar, A. (2005) hMOF histone acetyltransferase is required for histone H4 lysine 16 acetylation in mammalian cells. *Mol. Cell. Biol.*, **25**, 6798–6810.
5. Gupta, A., Guerin-Peyrou, T. G., Sharma, G. G. *et al.* (2008) The mammalian ortholog of Drosophila MOF that acetylates histone H4 lysine 16 is essential for embryogenesis and oncogenesis. *Mol. Cell. Biol.*, **28**, 397–409.
6. Gupta, A., Sharma, G. G., Young, C. S. *et al.* (2005) Involvement of human MOF in ATM function. *Mol. Cell. Biol.*, **25**, 5292–5305.
7. Hilfiker, A., Hilfiker-Kleiner, D., Pannuti, A. and Lucchesi, J. C. (1997) mof, a putative acetyl transferase gene related to the Tip60 and MOZ human genes and to the SAS genes of yeast, is required for dosage compensation in Drosophila. *EMBO J.*, **16**, 2054–2060.
8. Sterner, D. E. and Berger, S. L. (2000) Acetylation of histones and transcription-related factors. *Microbiol. Mol. Biol. Rev.*, **64**, 435–459.
9. Suka, N., Luo, K. and Grunstein, M. (2002) Sir2p and Sas2p opposingly regulate acetylation of yeast histone H4 lysine16 and spreading of heterochromatin. *Nat. Genet.*, **32**, 378–383.
10. Kumar, R., Hunt, C. R., Gupta, A. *et al.* (2011) Purkinje cell-specific males absent on the first (mMof) gene deletion results in an ataxia-telangiectasia-like neurological phenotype and backward walking in mice. *Proc. Natl Acad. Sci. USA,* **108**, 3636–3641.
11. Borrow, J., Stanton, V. P., Jr, Andresen, J. M. *et al.* (1996) The translocation t(8;16)(p11;p13) of acute myeloid leukaemia fuses a putative acetyltransferase to the CREB-binding protein. *Nat. Genet.*, **14**, 33–41.
12. Shiloh, Y. (1995) Ataxia-telangiectasia: closer to unraveling the mystery. *Eur. J. Hum. Genet.*, **3**, 116–138.
13. Bundey, S. (1994) Clinical and genetic features of ataxia-telangiectasia. *Int. J. Radiat. Biol.*, **66**, S23–S29.
14. Vorechovsky, I., Luo, L., Lindblom, A., Negrini, M., Webster, A. D., Croce, C. M. and Hammarstrom, L. (1996) ATM mutations in cancer families. *Cancer Res.*, **56**, 4130–4133.
15. Elson, A., Wang, Y., Daugherty, C. J., Morton, C. C., Zhou, F., Campos-Torres, J. and Leder, P. (1996) Pleiotropic defects in ataxia-telangiectasia protein-deficient mice. *Proc. Natl Acad. Sci. USA,* **93**, 13084–13089.
16. Gu, H., Marth, J. D., Orban, P. C., Mossmann, H. and Rajewsky, K. (1994) Deletion of a DNA polymerase beta gene segment in T cells using cell type-specific gene targeting. *Science*, **265**, 103–106.
17. Pandita, T. K. (1983) Effect of temperature variation on sister chromatid exchange frequency in cultured human lymphocytes. *Hum. Genet.*, **63**, 189–190.
18. Pandita, T. K. (1988) Assessment of the mutagenic potential of a fungicide Bavistin using multiple assays. *Mutat. Res.*, **204**, 627–643.
19. Pandita, T. K., Pathak, S. and Geard, C. R. (1995) Chromosome end associations, telomeres and telomerase activity in ataxia telangiectasia cells. *Cytogenet. Cell Genet.*, **71**, 86–93.
20. Pandita, T. K. (2006) Role of mammalian Rad9 in genomic stability and ionizing radiation response. *Cell Cycle*, **5**, 1289–1291.
21. Hunt, C. R., Dix, D. J., Sharma, G. G., Pandita, R. K., Gupta, A., Funk, M. and Pandita, T. K. (2004) Genomic instability and enhanced radiosensitivity in Hsp70.1- and Hsp70.3-deficient mice. *Mol. Cell. Biol.*, **24**, 899–911.
22. Pandita, T. K. (1986) Evaluation of Thimet 10-G for mutagenicity by 4 different genetic systems. *Mutat. Res.*, **171**, 131–138.
23. Pandita, T. K. (2003) A multifaceted role for ATM in genome maintenance. *Expert Rev. Mol. Med.*, **5**, 1–21.
24. Meyn, M. S. (1995) Ataxia-telangiectasia and cellular responses to DNA damage. *Cancer Res.*, **55**, 5991–6001.
25. Perez-Campo, F. M., Borrow, J., Kouskoff, V. and Lacaud, G. (2009) The histone acetyl transferase activity of monocytic leukemia zinc finger is critical for the proliferation of hematopoietic precursors. *Blood*, **113**, 4866–4874.
26. Liyanage, M., Weaver, Z., Barlow, C., Coleman, A., Pankratz, D. G., Anderson, S., Wynshaw-Boris, A. and Ried, T. (2000) Abnormal rearrangement within the alpha/delta T-cell receptor locus in lymphomas from Atm-deficient mice. *Blood*, **96**, 1940–1946.

27. Vacchio, M. S., Olaru, A., Livak, F. and Hodes, R. J. (2007) ATM deficiency impairs thymocyte maturation because of defective resolution of T cell receptor alpha locus coding end breaks. *Proc. Natl Acad. Sci. USA*, **104**, 6323–6328.
28. Oka, S., Mori, N., Matsuyama, S., Takamori, Y. and Kubo, K. (2000) Presence of B220 within thymocytes and its expression on the cell surface during apoptosis. *Immunology*, **100**, 417–423.
29. Shogren-Knaak, M., Ishii, H., Sun, J. M., Pazin, M. J., Davie, J. R. and Peterson, C. L. (2006) Histone H4-K16 acetylation controls chromatin structure and protein interactions. *Science*, **311**, 844–847.
30. Howard, M., Farrar, J., Hilfiker, M., Johnson, B., Takatsu, K., Hamaoka, T. and Paul, W. E. (1982) Identification of a T cell-derived b cell growth factor distinct from interleukin 2. *J. Exp. Med.*, **155**, 914–923.
31. Coffman, R. L., Seymour, B. W., Lebman, D. A. *et al.* (1988) The role of helper T cell products in mouse B cell differentiation and isotype regulation. *Immunol. Rev.*, **102**, 5–28.
32. Pandita, T. K. (2002) ATM function and telomere stability. *Oncogene*, **21**, 611–618.
33. Nagar, S., Smith, L. E. and Morgan, W. F. (2003) Characterization of a novel epigenetic effect of ionizing radiation: the death-inducing effect. *Cancer Res.*, **63**, 324–328.
34. Sowa, M. B., Goetz, W., Baulch, J. E. *et al.* (2010) Lack of evidence for low-LET radiation induced bystander response in normal human fibroblasts and colon carcinoma cells. *Int. J. Radiat. Biol.*, **86**, 102–113.
35. Morgan, W. F., Hartmann, A., Limoli, C. L., Nagar, S. and Ponnaiya, B. (2002) Bystander effects in radiation-induced genomic instability. *Mutat. Res.*, **504**, 91–100.
36. Pandita, R. K., Sharma, G. G., Laszlo, A. *et al.* (2006) Mammalian Rad9 plays a role in telomere stability, S- and G2-phase-specific cell survival, and homologous recombinational repair. *Mol. Cell. Biol.*, **26**, 1850–1864.
37. Sharma, G. G., Hwang, K. K., Pandita, R. K. *et al.* (2003) Human heterochromatin protein 1 isoforms HP1(Hsalpha) and HP1(Hsbeta) interfere with hTERT-telomere interactions and correlate with changes in cell growth and response to ionizing radiation. *Mol. Cell. Biol.*, **23**, 8363–8376.
38. Biedermann, K. A., Sun, J. R., Giaccia, A. J., Tosto, L. M. and Brown, J. M. (1991) scid mutation in mice confers hypersensitivity to ionizing radiation and a deficiency in DNA double-strand break repair. *Proc. Natl Acad. Sci. USA*, **88**, 1394–1397.
39. Pandita, T. K. and Richardson, C. (2009) Chromatin remodeling finds its place in the DNA double-strand break response. *Nucleic Acids Res.*, **37**, 1363–1377.